

Intermediate-valence behavior of the transition-metal oxide $\text{CaCu}_3\text{Ru}_4\text{O}_{12}$

Alexander Krimmel, Armin Günther, W. Kraetschmer, H. Dekinger, Norbert Büttgen, Volker Eyert, Alois Loidl, D. V. Sheptyakov, Ernst-Wilhelm Scheidt, Wolfgang Scherer

Angaben zur Veröffentlichung / Publication details:

Krimmel, Alexander, Armin Günther, W. Kraetschmer, H. Dekinger, Norbert Büttgen, Volker Eyert, Alois Loidl, D. V. Sheptyakov, Ernst-Wilhelm Scheidt, and Wolfgang Scherer. 2009. "Intermediate-valence behavior of the transition-metal oxide $\text{CaCu}_3\text{Ru}_4\text{O}_{12}$." *Physical Review B* 80 (12): 121101(R).
<https://doi.org/10.1103/physrevb.80.121101>.



Intermediate-valence behavior of the transition-metal oxide $\text{CaCu}_3\text{Ru}_4\text{O}_{12}$

A. Krimmel, A. Günther, W. Kraetschmer, H. Dekinger, N. Büttgen, V. Eyert, and A. Loidl
Center for Electronic Correlations and Magnetism, University of Augsburg, 86135 Augsburg, Germany

D. V. Sheptyakov

Laboratory for Neutron Scattering, ETH Zürich and PSI Villigen, CH-5232 Villigen, Switzerland

E.-W. Scheidt and W. Scherer

CPM, Institute of Physics, University of Augsburg, 86135 Augsburg, Germany

(Received 6 April 2009; revised manuscript received 12 August 2009; published 22 September 2009)

The transition-metal oxide $\text{CaCu}_3\text{Ru}_4\text{O}_{12}$ with perovskite-type structure shows characteristic properties of an intermediate-valence system. The temperature-dependent susceptibility exhibits a broad maximum around 150–160 K. At this temperature, neutron powder diffraction reveals a small but significant volume change whereby the crystal structure is preserved. Moreover, the temperature-dependent resistivity changes its slope. NMR Knight shift measurements of Ru reveal a cross-over from high temperature paramagnetic behavior of localized moments to itinerant band states at low temperatures. Additional density-functional theory calculations can relate the structural anomaly with the d -electron number. The different experimental and calculational methods result in a mutually consistent description of $\text{CaCu}_3\text{Ru}_4\text{O}_{12}$ as an intermediate-valent system in the classical sense of having low-energy charge fluctuations.

DOI: [10.1103/PhysRevB.80.121101](https://doi.org/10.1103/PhysRevB.80.121101)

PACS number(s): 71.27.+a, 65.40.Ba, 75.20.Hr

A-site ordered perovskite oxides of stoichiometry $\text{AA}'_3\text{B}_4\text{O}_{12}$ show a variety of fascinating physical properties. $\text{CaCu}_3\text{Ti}_4\text{O}_{12}$ has been extensively studied with respect to colossal dielectric properties^{1,2} and $\text{CaCu}_3\text{Mn}_4\text{O}_{12}$ is a ferromagnet with an ordering temperature as high as $T_C=360$ K and large magnetoresistance.^{3,4} On the other hand, the ruthenates $\text{ACu}_3\text{Ru}_4\text{O}_{12}$ ($A=\text{Na}, \text{Ca}, \text{La}$) are metallic Pauli paramagnets⁵ displaying valence degeneracy.⁶ Moreover, they show enhanced Sommerfeld coefficients indicative of strong electronic correlations.^{7–10} Recently, $\text{CaCu}_3\text{Ru}_4\text{O}_{12}$ was shown to exhibit heavy-fermion-like properties.⁸ In analogy to CeSn_3 , a broad maximum in the susceptibility was taken as a signature of the Kondo temperature of about 200 K and a moderately enhanced Sommerfeld coefficient of $\gamma=85$ mJ/(f.u. mol K^2) was observed.⁸ Conventional f -electron based heavy-fermion states are formed via hybridization between two different electronic subsystems, namely, localized f electrons and band states of conduction electrons.¹¹ This results in a highly enhanced density of states (DOS) at the Fermi level E_F (Abrikosov-Suhl resonance) and a concomitantly quasiparticle renormalization described by an enhanced effective electronic mass $m^*/m_e = 10^2 - 10^3$. However, it has been demonstrated that heavy-fermion behavior should also occur in transition-metal oxides upon approaching a metal-insulator transition.¹²

On the basis of x-ray spectroscopic measurements a direct analogy of $\text{CaCu}_3\text{Ru}_4\text{O}_{12}$ to conventional f -electron heavy fermions was reported based on localized magnetic moments of the Cu^{2+} ions and itinerant d -electrons originating from strong Ru-O hybridization.¹³ Localized and itinerant electrons are supposed to be coupled antiferromagnetically by the Kondo mechanism.¹³ Recently, heat-capacity and NMR/nuclear quadrupole resonance (NQR) measurements revealed non-Fermi-liquid properties of $\text{CaCu}_3\text{Ru}_4\text{O}_{12}$ at very low temperatures.⁹ Moreover, a comprehensive study of $\text{ACu}_3\text{Ru}_4\text{O}_{12}$ ($A=\text{Na}, \text{Na}_{0.5}\text{Ca}_{0.5}, \text{Ca}, \text{Ca}_{0.5}\text{La}_{0.5}, \text{La}$) (Ref. 10)

established large Sommerfeld coefficients $\gamma = 75 - 136$ mJ/(f.u. mol K^2) for all investigated compounds, whereas a broad maximum in the susceptibility was observed only for $\text{CaCu}_3\text{Ru}_4\text{O}_{12}$. Evidently, $\text{CaCu}_3\text{Ru}_4\text{O}_{12}$ represents a particular case among electronically correlated ruthenate compounds. Most recently, Kato *et al.* studied $\text{CaCu}_3\text{Ru}_4\text{O}_{12}$ by NMR experiments.¹⁴ Following Ref. 14, the temperature-dependent relaxation rate excludes a localized magnetic moment at the Cu site. Here we provide experimental evidence that $\text{CaCu}_3\text{Ru}_4\text{O}_{12}$ is an outstanding example of a transition-metal oxide which can be classified as an intermediate-valent (IV) system in the classical sense of having low-energy charge fluctuations.

Polycrystalline samples of $\text{CaCu}_3\text{Ru}_4\text{O}_{12}$ were synthesized by a solid-state reaction as described previously.⁹ The samples were characterized by x-ray powder diffraction and revealed single phase material without any indications of spurious phases. Neutron powder-diffraction measurements were performed on the high resolution powder diffractometer for thermal neutrons (HRPT) at the Paul Scherrer Institut, Switzerland. The diffraction patterns were refined by standard Rietveld analysis employing the FULLPROF program suite.¹⁵ The crystal structure of $\text{CaCu}_3\text{Ru}_4\text{O}_{12}$ can be considered as a $2 \times 2 \times 2$ superstructure of the parent perovskite structure ABO_3 . It is described by cubic symmetry with space group $Im\bar{3}$ and atomic positions of Ca at (0, 0, 0), Cu at $(\frac{1}{2}, 0, 0)$, Ru at $(\frac{1}{4}, \frac{1}{4}, \frac{1}{4})$, and O at $(x, y, 0)$. At $T=1.6$ K, refined structural parameters are the lattice constant $a = 7.41221(5)$ Å and the oxygen positional parameters $x = 0.17478(13)$ and $y = 0.30746(13)$. These values comply with those reported in the literature.^{5,16} The temperature-dependent lattice constant as resulting from the refinements is shown in Fig. 1. In this figure, the error bars are smaller than the symbol size. A small ($\approx 10^{-3}$) but significant and sharp anomaly is evident at $T_V=150$ K. At low temperatures

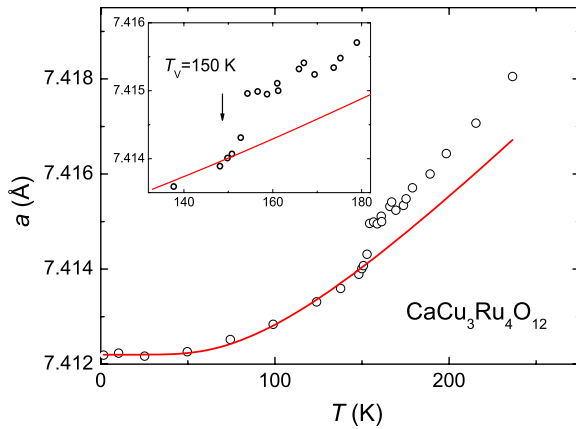


FIG. 1. (Color online) Temperature dependence of the lattice constant a of $\text{CaCu}_3\text{Ru}_4\text{O}_{12}$ as resulting from the Rietveld refinements of the neutron powder-diffraction measurements. The solid line is a fit according to a usual anharmonic behavior described in the text.

$T \leq 150$ K, the lattice constant $a(T)$ was fitted assuming an ordinary anharmonic behavior according to $a(T) = a_0 + \Delta a / [1 - \exp(-\theta_D/T)]$ with a Debye temperature of $\Theta_D = 307$ K. The result is shown as a solid line in Fig. 1. This fit nicely illustrates the abrupt expansion of the unit-cell volume. Cycling the temperature revealed full reversibility without hysteresis. This is in contrast to the behavior of the homologue compound $\text{PrCu}_3\text{Ru}_4\text{O}_{12}$ which does not show such a structural anomaly (not shown). The Rietveld analysis shows that the crystal structure (lattice symmetry and atomic positions) remains unchanged. Within the experimental accuracy, the oxygen positional parameters of $\text{CaCu}_3\text{Ru}_4\text{O}_{12}$ are constant. The metal-oxygen distance show a smooth temperature dependence whereas all metal-metal distances reveal an anomalous expansion close to 150 K. A structural anomaly in form of a sudden lattice expansion, whereby the crystal structure is fully preserved, clearly points to an electronic origin in form of valence fluctuations. The change in the unit-cell volume is consistent with a transition from localized $4d$ electrons at high temperatures ($T > T_V$) to itinerant band states at low temperatures ($T < T_V$). Moreover, the temperature of the structural transition of $\text{CaCu}_3\text{Ru}_4\text{O}_{12}$ coincides reasonably well with the temperature of the broad maximum of the magnetic susceptibility, thus confirming an electronic origin.

The heat capacity $C(T)/T$ versus T of $\text{CaCu}_3\text{Ru}_4\text{O}_{12}$ is shown in Fig. 2. It exhibits a conventional behavior of metallic Fermi liquids for $T > 2$ K according to $C(T) = \gamma T + \beta T^3$. Non-Fermi-liquid properties were observed⁹ for $T < 2$ K. The phononic contribution results in a Debye temperature of $\Theta_D = 451$ K which is considerably enhanced when compared to that determined from the low-temperature thermal expansion. The electronic part is described by a Sommerfeld coefficient of $\gamma = 92 \pm 2$ mJ/(f.u. mol K²). The right side inset shows the specific heat of $\text{CaCu}_3\text{Ru}_4\text{O}_{12}$ on an expanded scale in a restricted temperature range $135 \leq T \leq 160$ K around the anomalous volume transition. A small but significant maximum in $C/T(T)$ is seen. Heating and cooling runs (corresponding to open blue squares and open

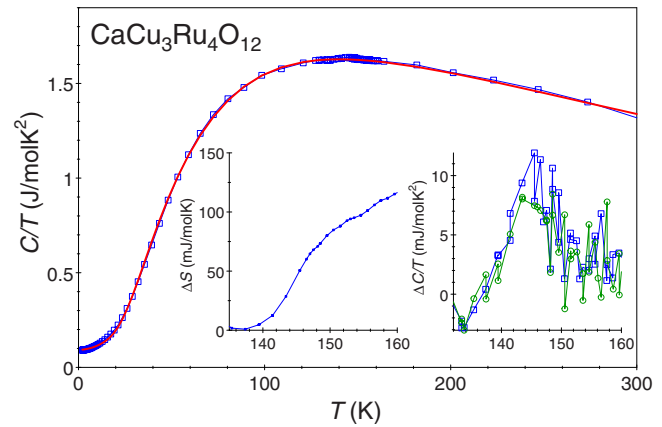


FIG. 2. (Color online) Heat capacity C/T versus T of $\text{CaCu}_3\text{Ru}_4\text{O}_{12}$. A small but significant peak is observed in the temperature range $135 < T < 160$ K. To account for the phonon contributions, the data were fitted by a Debye term and four Einstein modes (solid red line). The right-hand inset shows the heat-capacity anomaly on an expanded scale for heating (open blue squares) and cooling (open green circles) evidencing the absence of hysteresis. The left hand inset shows the associated entropy change of about 70 mJ/(f.u. mol K).

green circles, respectively) demonstrate a complete reversibility of the volume transition without any indications of hysteresis, as observed in the neutron powder-diffraction measurements. This points toward a second-order phase transition. The associated entropy is shown in the left side inset and amounts to approximately 70 mJ/(f.u. mol K).

Electronic structure calculations¹⁷ gave evidence for strong covalent bonding between metal d and oxygen p electrons. While the Ru-O bonds determine the size of the RuO_6 octahedra, the Cu-O bonds dominate the octahedral tilting. The partial DOS of Cu shows large peaks in the region $-2 > E > -3$ eV below the Fermi energy and some residual states above E_F due to hybridization effects. This implies a rather closed $3d$ shell and is consistent with the absence of a localized magnetic moment at the Cu site in agreement with experiments.¹⁴ In the region around the Fermi energy, the electronic states derive mainly from broader Ru $4d$ bands although covalent bonding leads to finite oxygen $2p$ contributions at E_F .¹⁷ Therefore, a significant contribution of the Kondo effect at the Cu site for the mass renormalization can be excluded due to the absence of a magnetic moment. The DOS at E_F is dominated by Ru, whereas the Cu contribution is negligible.¹⁷ This is experimentally confirmed by NMR (Knight shift K) and NQR (spin-lattice relaxation rate $1/T_1$) measurements on ^{63}Cu , ^{99}Ru , and ^{101}Ru , respectively. The bottom frame of Fig. 3 shows the temperature-dependent spin-lattice relaxation rate $1/T_1$ which reveals an enhanced Korringa behavior for ^{101}Ru [as compared to pure Ru metal (Ref. 18)] reflecting a high DOS at the Fermi level, whereas $1/T_1$ of ^{63}Cu is close to but slightly below that of pure Cu metal (Ref. 19).

The top frame of Fig. 3 shows the Knight shift K of Cu (left scale) and Ru (right scale), respectively. The Knight shift of Cu is positive despite the fact that the core electron polarization provides negative values. This excludes a sig-

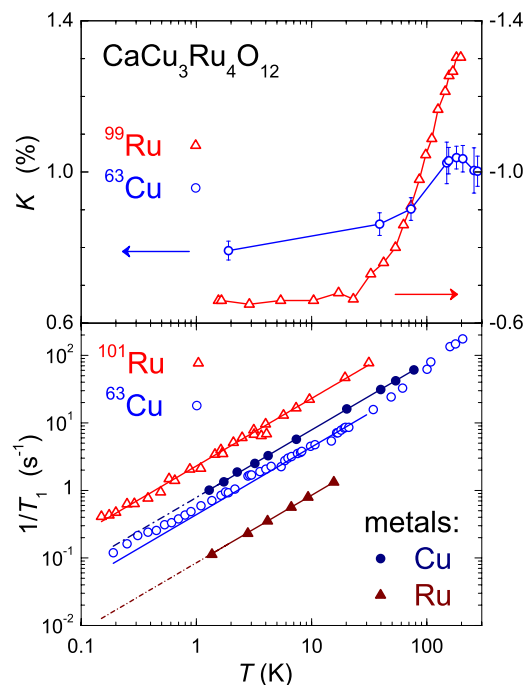


FIG. 3. (Color online) The top frame shows the Knight shift K of Cu (blue circles, left scale) and Ru (red triangles, right scale), respectively. Please note the different sign of the two scales. The bottom frame shows the spin-lattice relaxation rate $1/T_1$ of $\text{CaCu}_3\text{Ru}_4\text{O}_{12}$ for ^{63}Cu and ^{101}Ru , respectively. The full lines represent fits to the data according to a Korringa law. For comparison, the relaxation rates of pure Cu and Ru metal are also shown.

nificant contribution of d electrons to the Knight shift at the Cu site. The temperature dependence of $^{\text{Cu}}K$ is weak and follows the magnetic susceptibility. Taking into account the absence of a localized magnetic moment at the Cu site, we conclude that $^{\text{Cu}}K$ reflects the temperature dependence of a transferred field. On the other hand, the Knight shift at the Ru site reveals negative values due to the Ru core-polarization effects. This points to a dominant contribution of $4d$ electrons of Ru ions to the magnetic behavior of $\text{CaCu}_3\text{Ru}_4\text{O}_{12}$. Moreover, $^{\text{Ru}}K$ exhibits a more pronounced temperature dependence evidencing a stronger moment compensation upon cooling. Toward the lowest temperatures, the Knight shift at the Ru site becomes temperature independent. This behavior hallmarks the crossover from paramagnetism of localized electrons to Pauli paramagnetism of itinerant band states.

We further note that the temperature-dependent resistivity changes slope around 150–160 K with a steeper decline in the low-temperature region.⁹ Such a behavior is expected for a mixed-valence transition when a fraction of originally localized $4d$ electrons becomes (partly) itinerant.

New *ab initio* electronic structure calculations of $\text{CaCu}_3\text{Ru}_4\text{O}_{12}$ were performed with the structural input parameters obtained by the refinements of the neutron powder-diffraction measurements. The calculations are based on density-functional theory (DFT) and the local-density approximation (LDA). They were performed using a scalar-relativistic implementation of the augmented spherical wave (ASW) method.^{20,21} In the present work, a full-potential ver-

sion of the ASW method was employed in which the electron density and related quantities are given by spherical harmonics expansions inside the muffin-tin spheres. In the remaining interstitial region, a representation in terms of atom-centered Hankel functions is used. The calculated partial densities of states do not show any significant changes as compared to the previous study.¹⁷ The calculated d -electron number n_d of Ru has an almost half-integral value of 5.5 which reflects a strongly covalent Ru-O bond thus pointing toward intermediate valency of the Ru ions. A qualitative difference between a low-temperature ($T \leq 125$ K) region with almost constant d -electron number and a high-temperature ($T \geq 150$ K) regime with a roughly linear increase in n_d can be distinguished.

It is evident that the transition between the high- T and low- T behavior of $\text{CaCu}_3\text{Ru}_4\text{O}_{12}$ involves only small changes in the electronic structure. This is reflected in the small value of 10^{-3} of the abrupt volume change at $T_V = 150$ K (see Fig. 1). Moreover, the calculated variations of the d -electron occupancies of about 10^{-3} are two orders of magnitude smaller than in traditional f -electron-based intermediate-valence systems. The relaxation rate and the Knight shift in recent NMR measurements¹⁴ were explained in terms of a two-band model for the markedly different high- T state above the susceptibility maximum around 160 K and the low- T behavior below about 20 K. A strong hybridization corresponding to increasing correlations between Cu and Ru electrons would enable an effective charge transfer between these two bands.¹⁴ Charge order, charge localization, and valence transitions are often observed in transition-metal oxides, mainly in manganites, vanadates and ruthenates. As a prototypical example we discuss the valence transition which has recently been reported in $\text{LaCu}_3\text{Fe}_4\text{O}_{12}$ which is isostructural to $\text{CaCu}_3\text{Ru}_4\text{O}_{12}$.²² On cooling, the Cu ions of this compound undergo a valence transition from Cu^{2+} to Cu^{3+} accompanied by a metal to insulator transition and a striking volume change. The corresponding volume change due to this integral change in valence states is of the order of 1% compared to a volume change of 0.04% in $\text{CaCu}_3\text{Ru}_4\text{O}_{12}$ where only a small fraction of d electrons is involved. The susceptibility of the $AA'B_4O_{12}$ oxides toward charge disproportion with associated structural and magnetic instabilities was also discussed in the case of $\text{CaCu}_3\text{Fe}_4\text{O}_{12}$ recently.²³ However, in all cases different but integral valence states have been observed.

The d -electron correlations in transition-metal oxides are traditionally taken into account by a Mott-Hubbard approach. The relevant energy scale is determined by the on-site Coulomb repulsion U of the order of eV. Therefore, transition-metal oxides usually exhibit high-energy electronic fluctuations. Many years ago, Allen²⁴ discussed the possibility of valence fluctuations in narrow-band oxides. The starting point was the lattice Anderson Hamiltonian and its relation to a Hubbard band description usually applied for transition-metal compounds. Valence fluctuations become possible if the energy E_g of the transition $d^n \rightarrow d^{n+1}$ tends to zero, and it was suggested that this situation may be realized near a metal-insulator or metal-semimetal transition. The required large value of the hybridization V seems to favor sulfur (or even selenide) compounds as compared to oxides. In

the present case of $\text{CaCu}_3\text{Ru}_4\text{O}_{12}$, the strong covalent Ru-O bond results from a strong hybridization between ruthenium $4d$ and oxygen $2p$ electrons necessary for IV behavior. The larger spatial extent of $4d$ electron wave functions as compared to the narrower $3d$ electron bands seems to be a prerequisite for a sufficiently strong hybridization to result in IV properties but, on the other hand, weakens electronic correlations. To look for further IV systems, one therefore should consider $4d$ transition-metal oxides with metallic conductivity and enhanced Sommerfeld coefficients. These conditions seem to be realized at best among the ruthenates.

In summary, the temperature-dependent magnetic susceptibility, NMR spin-lattice relaxation rate $1/T_1$ and Knight shift measurements of Ru and Cu, the anomalous volume

transition at $T_V=150$ K found in neutron powder diffraction, which is confirmed by a corresponding anomaly in the heat capacity, as well as electronic structure calculations provide a mutually consistent description of $\text{CaCu}_3\text{Ru}_4\text{O}_{12}$ as the first example of a transition-metal oxide with IV properties in the classical sense of having d -electron fluctuations. Other ruthenates seem to be the most promising candidates to find further examples of this class of materials.

This work was supported by the Deutsche Forschungsgemeinschaft (DFG) via research unit 960 “Quantum Phase Transitions,” Sonderforschungsbereich 484 (Augsburg), DFG Contract No. SCHE487/7 and by the project COST P16 ECOM of the European Union.

-
- ¹C. C. Homes, T. Vogt, S. M. Shapiro, S. Wakimoto, and A. P. Ramirez, *Science* **293**, 673 (2001).
- ²P. Lunkenheimer, R. Fichtl, S. G. Ebbinghaus, and A. Loidl, *Phys. Rev. B* **70**, 172102 (2004) and references therein.
- ³Z. Zeng, M. Greenblatt, M. A. Subramanian, and M. Croft, *Phys. Rev. Lett.* **82**, 3164 (1999).
- ⁴R. Weht and W. E. Pickett, *Phys. Rev. B* **65**, 014415 (2001).
- ⁵M. Labeau, B. Bochu, J. C. Joubert, and J. Chenavas, *J. Solid State Chem.* **33**, 257 (1980).
- ⁶M. A. Subramanian and A. W. Sleight, *Solid State Sci.* **4**, 347 (2002).
- ⁷A. P. Ramirez, G. Lawes, D. Li, and M. A. Subramanian, *Solid State Commun.* **131**, 251 (2004).
- ⁸W. Kobayashi, I. Terasaki, J.-i. Takeya, I. Tsukada, and Y. Ando, *J. Phys. Soc. Jpn.* **73**, 2373 (2004).
- ⁹A. Krimmel, A. Gunther, W. Kraetschmer, H. Dekinger, N. Buttgen, A. Loidl, S. G. Ebbinghaus, E. W. Scheidt, and W. Scherer, *Phys. Rev. B* **78**, 165126 (2008).
- ¹⁰S. Tanaka, N. Shimazui, H. Takatsu, S. Yonezawa, and Y. Maeno, *J. Phys. Soc. Jpn.* **78**, 024706 (2009).
- ¹¹N. Grewe and F. Steglich, *Handbook on the Physics and Chemistry of Rare Earth*, edited by K. A. Gschneidner, Jr. and L. L. Eyring (Elsevier, Amsterdam, 1991), Vol. 14, p. 343.
- ¹²H.-A. Krug von Nidda, R. Bulla, N. Büttgen, M. Heinrich, and A. Loidl, *Eur. Phys. J. B* **34**, 399 (2003).
- ¹³T. T. Tran, K. Takubo, T. Mizokawa, W. Kobayashi, and I. Terasaki, *Phys. Rev. B* **73**, 193105 (2006).
- ¹⁴H. Kato, T. Tsuruta, M. Matsumura, T. Nishioka, H. Sakai, Y. Tokunaga, S. Kambe, and R. E. Walstedt, *J. Phys. Soc. Jpn.* **78**, 054707 (2009).
- ¹⁵J. Rodriguez-Carvajal, *Physica B* **192**, 55 (1993).
- ¹⁶S. G. Ebbinghaus, A. Weidenkaff, and R. J. Cava, *J. Solid State Chem.* **167**, 126 (2002).
- ¹⁷U. Schwingenschlögl, V. Eyert, and U. Eckern, *Chem. Phys. Lett.* **370**, 719 (2003).
- ¹⁸H. Mukuda, K. Ishida, Y. Kitaoka, K. Asayama, R. Kanno, and M. Takano, *Phys. Rev. B* **60**, 12279 (1999).
- ¹⁹M. Hanabusa and T. Kushida, *Phys. Rev. B* **5**, 3751 (1972).
- ²⁰V. Eyert, *Int. J. Quantum Chem.* **77**, 1007 (2000).
- ²¹V. Eyert, *The Augmented Spherical Wave Method: A Comprehensive Treatment*, Lecture Notes Phys. Vol. 719 (Springer, Berlin, Heidelberg, 2007).
- ²²Y. W. Long, N. Hayashi, T. Saito, M. Azuma, S. Muranaka, and Y. Shimakawa, *Nature (London)* **458**, 60 (2009).
- ²³X. Hao, Y. Xu, F. Gao, D. Zhou, and J. Meng, *Phys. Rev. B* **79**, 113101 (2009).
- ²⁴J. W. Allen, *J. Magn. Magn. Mater.* **47-48**, 168 (1985).